

Supporting Information

Fe–N–C Electrocatalysts in the Oxygen and Nitrogen Cycles in Alkaline Media: The Role of Iron Carbide

Tomer Y. Burshtein, Denial Aias, Jin Wang, Matan Sananis, Eliyahu M. Farber, Oz M. Gazit, Ilya Grinberg, David Eisenberg*

Synthesis of carbide-rich materials

Carbide **A** was synthesized by pyrolyzing Fe₃O₄ NPs with oleic acid (OLA), which were prepared following the procedure of Park et al.¹ The crude oily mixture of Fe₃O₄ NPs-OLA was transferred to a quartz boat and pyrolyzed under Ar using the following program: 12 °C /min to 700 °C with 4-hour hold, then naturally cool to room temperature.

Carbide **B** was synthesized according to Fletcher et al.² In deionized water (DI, 240 mL), FeCl₂·4H₂O (0.6 g, 3 mmol) and polyvinylpyrrolidone (20,000 MW, 0.33 g, 3 mmol) were added and stirred to complete dissolution. Separately, K₃[Fe(CN)₆] (0.99 g, 3 mmol) was dissolved in DI (60 mL). The K₃[Fe(CN)₆] solution was added drop-wise to the FeCl₂-PVP solution under vigorous stirring. The solution was stirred for a further 30 minutes, then acetone (300 mL) was added. The Prussian blue particles were washed with acetone three times and separated by centrifugation. After evaporating the remaining acetone, the solid was weighed and transferred to a large beaker with methanol (300 mL). MgO NPs powder (20 nm) was added (1:1 mass ratio to Prussian blue particles) and stirred while evaporating the methanol at 50 °C. After full evaporation, the pale blue solid was further dried at 70 °C in air for 24 hours. The solid was transferred to a quartz boat and pyrolyzed under Ar by the following program: 5 °C/min to 800 °C with a 1-hour hold. After cooling naturally to room temperature, the matt-black powder was washed overnight in Na₂EDTA solution (7% molar excess to MgO, 0.2 M Na₂EDTA) to remove the MgO. The black solid was washed in DI and separated by centrifugation. The final product was obtained by washing the solid in 10 mL 30% H₂O₂ overnight, to remove amorphous carbon.

Carbide **C** was obtained by a solid-gas reaction, following Malina et al.³ b-Fe₂O₃ was synthesized by a literature method⁴, and then mixed with MgO at a 1:1 mass ratio and ground to a fine powder. The mixed powder was heated up to 400 °C with a heating rate 10 °C/min under Ar (50 mL/min) and was held at 400 °C for 1 hour. Then the sample was held at 400 °C in 10 v:v% CO/He (50 mL/min) for 40 minutes, then it was heated to 625 °C at 10 °C/min and was held at that temperature for 10 hours under 10 v:v% CO/He (50 mL/min). The product was cooled to room temperature under He flow, followed by washing overnight in Na₂EDTA solution (1:1 molar ratio to MgO, 0.2 M Na₂EDTA) to remove the MgO.

Carbide **D** was synthesized using a procedure by Giordano et al.⁵ In a beaker, FeCl₂·4H₂O (0.8 g, 4 mmol) was added to 40 mL absolute ethanol and stirred to full dissolution, giving a dark orange solution. Fe(CO)₅ (0.26 mL, 2 mmol) was added with a syringe, followed by slow addition of urea (1.08 g, 9 mmol). The solution was reduced to ~ 20 mL by heating on a hotplate, after which it was transferred to a quartz boat. After complete evaporation of the ethanol, a dark red gel formed. Under Ar flow, the boat was transferred to a tube furnace and heated at 12 °C/min to 700 °C, where it was held for 2 hours. After cooling naturally to room temperature, the gray powder was kept under Ar, to prevent the slow oxidation of Fe₃C.

Carbide **E** was purchased commercially (99%, American Elements, USA).

Material characterization

Characterization was performed using powder X-ray diffraction (XRD, Rigaku SmartLab), high-resolution scanning electron microscopy (HRSEM, Zeiss-ultra+, 3 kV), high-resolution transmission electron microscopy (HRTEM, FEI Tecnai and FEI Titan Themis, 200 kV), X-ray photoelectron spectroscopy (XPS, UHV ~ 2·10⁻¹⁰ torr using a Versa-probe III, PHI Instruments, 100 mm beam size, energy pass = 224 eV, step size = 0.4 eV, dwell time = 20 ms). ICP-MS used a CHN analyzer of the brand Elementar model Vario Mikro Cube. The elements Fe, Mg and Na were determined by us after an acid digestion on an ICP-OES of the brand Spectro Model Spectro Arcos. Chlorine was determined with an ion chromatography of the brand Metrohm Model 883 Plus after a combustion digestion. Particle size was determined manually from the HRSEM and HRTEM micrographs using ImageJ software.

Electrochemical procedures

Electrocatalytic hydrazine oxidation (HzOR) and oxygen reduction reaction (ORR) experiments were performed at room temperature in a three-electrode cell connected to a bipotentiostat (BioLogic 600). Catalyst-coated glassy carbon electrode (GCE), a graphite rod and a standard calomel electrode were used as working, counter and reference electrodes, respectively. For the catalyst ink, 10 mg of the Fe₃C-rich sample (or 1 mg of the washed samples) was dispersed in a mixture of 200 μ L ethanol, 800 μ L of DI water and 10 μ L of Nafion solution in IPA (0.5 wt%) and sonicated for 30 minutes. 20 μ L of the ink were deposited on GCE ($A = 0.1962 \text{ cm}^2$) and dried at 50 $^{\circ}\text{C}$ in air. The mass loading on the working electrode was 0.198 mg (0.0198 mg for washed samples). N₂-purged 1M KOH (pH=14) electrolyte solutions employed for HzOR experiments, and 0.1M KOH (pH=13) for ORR experiments. Cyclic voltammetry was carried at a potential range from -0.9 to 0.1 V (vs. SCE) for HzOR experiments, and RRDE linear sweep voltammetry was carried at a potential range from 0 to -1 V (vs. SCE) and 2400–600 rpm rotation rate for ORR experiments. Prior to O₂/N₂H₄ addition, a wetting sequence was performed by cycling the electrodes in the forementioned potentials.

Electrochemical active surface area (ECSA) measurements were performed from the double layer capacitance of the materials. The capacitance was determined from the CV cycles at 8 scan rates (5, 10, 20, 50, 100, 250 mV s^{-1}) at a small potential window of -0.2 V to 0 V (vs. SCE) in 1M KOH, N₂-purged solutions, where no Faradaic processes are occurring. The following equation was used:

$$A_{ECSA} = \frac{\text{Double layer capacitance}}{40 \mu\text{F cm}^{-2}}$$

this calculation assumes a typical value of 40 mF cm^{-2} for the surface-area normalized capacitance associated with double-layer charging.⁶

Additional micrographs

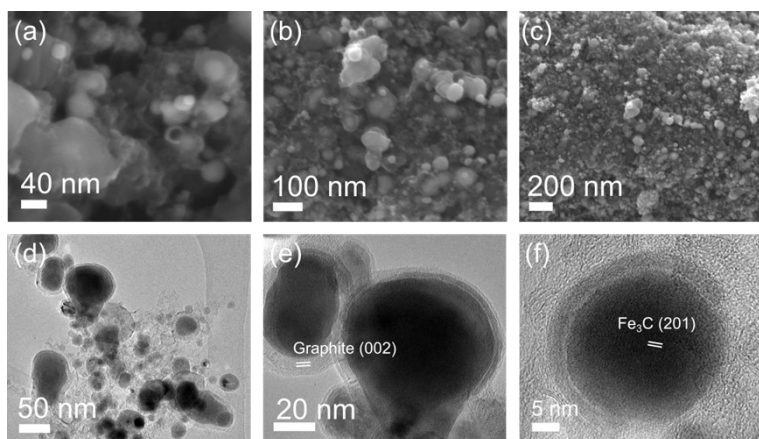


Figure S1. Carbide A electron micrographs. (a–c) HRSEM; (d–f) HRTEM of carbide nanoparticles, including crystal lattice spacing identification.

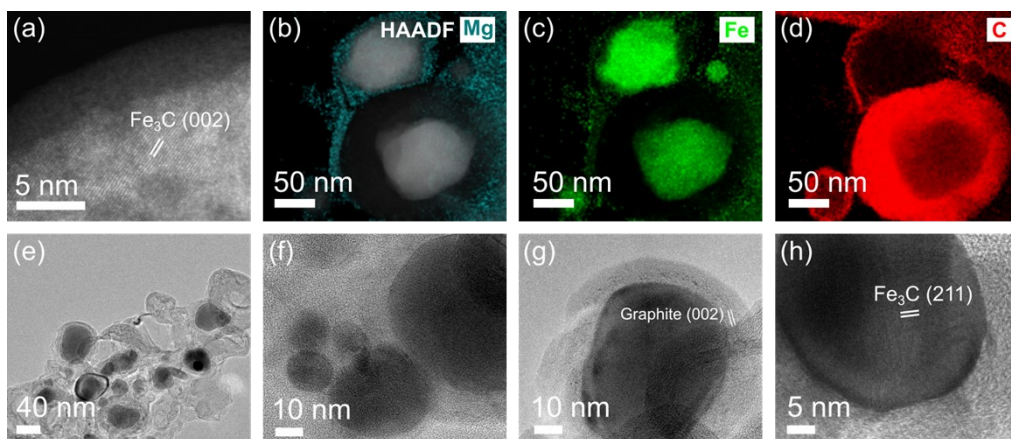


Figure S2. Carbide B electron micrographs. (a) HAADF-STEM crystal lattice spacing identification; (b–d) elemental mapping; (e–f) HRTEM showing particles in carbon support, (g) graphite lattice and (h) Fe₃C lattice. The Mg comes from the MgO anti-sintering additive, and was mostly washed out by EDTA.

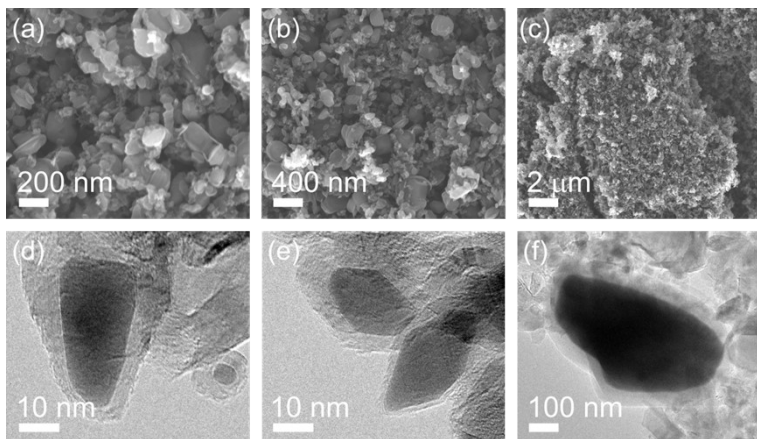


Figure S3. Carbide C electron micrographs. (a–c) HRSEM; (d–f) HRTEM of carbide nanoparticles

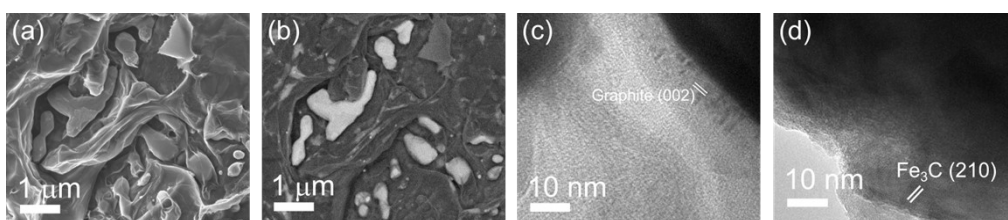


Figure S4. Carbide D electron micrographs. (a) SEM, secondary electrons, (b) SEM, back-scattered electrons, (c) HRSEM, secondary electrons, (d) HRSEM, back-scattered electrons. HRTEM of (e) particle free-carbon layers, (f) Fe_3C particles covered in carbon layers, (g) graphite layers wrapping a Fe_3C particle, (h) Fe_3C crystalline layers.

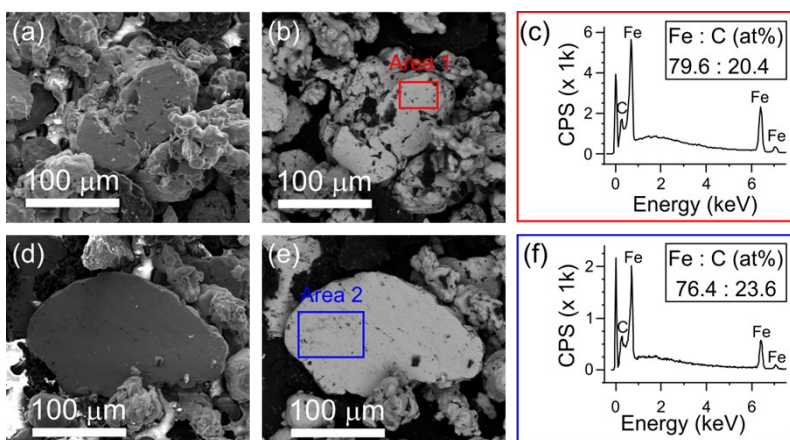


Figure S5. Carbide E (a, d) SE and (b, e) BSE SEM micrographs; dark regions are carbon rich. (c, f) EDS spectra of different regions.

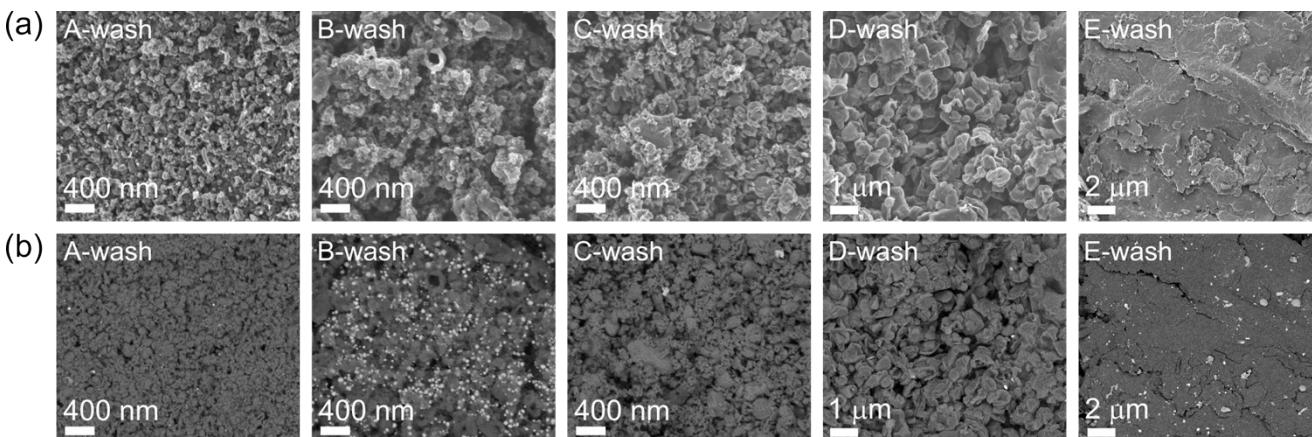


Figure S6. (a) HRSEM and (b) BSE HRSEM micrographs of A-/B-/C-/D-/E-wash carbides. Bright spots in the (b) row correspond to dense Fe_3C particles remaining after HCl wash.

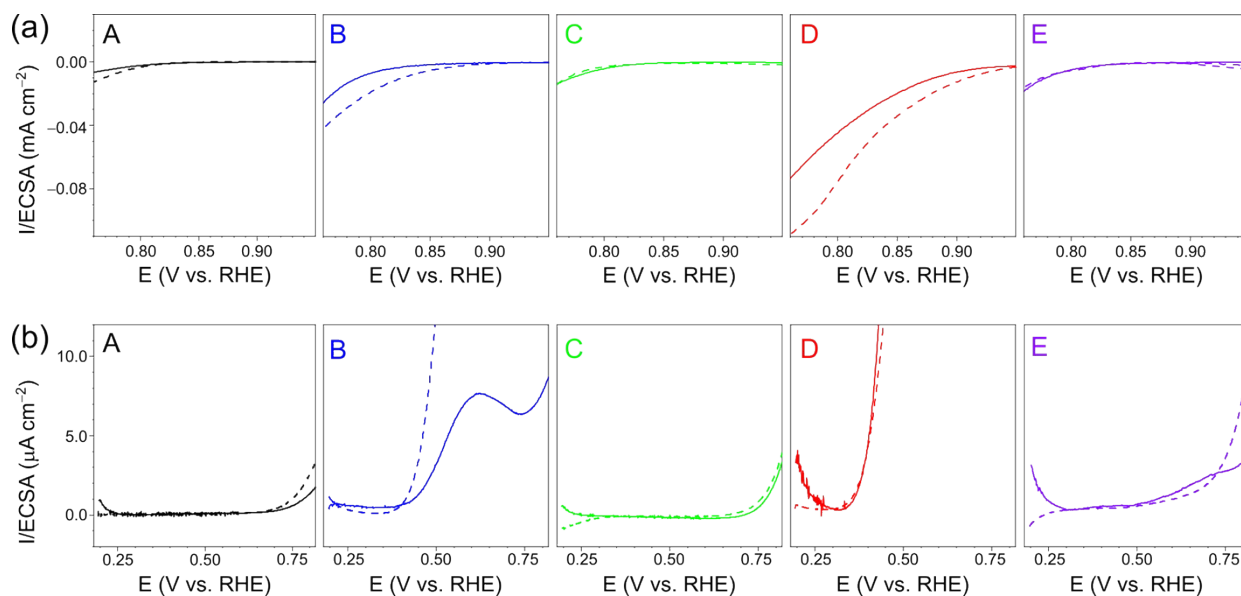


Figure S7. Linear sweep voltammograms of materials A–E before (solid line) and after (dashed line) the acid wash, corrected for absolute ECSA of the powder electrode, and thus stressing the similarity in onset potentials. (a) ORR, (b) HzOR.

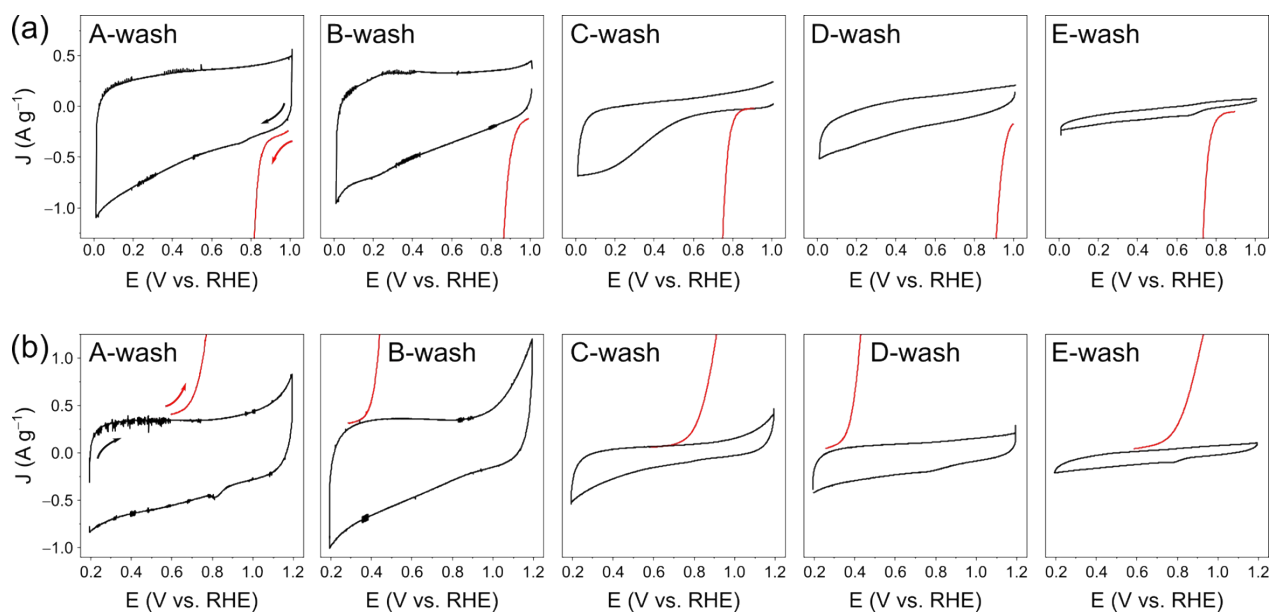


Figure S8. Voltammograms of materials A–E-wash in the absence of (a) O₂ and (b) N₂H₄ (black line, CV) and in the presence of O₂ / N₂H₄ (red line, LSV). Arrows point to the scan direction. Experimental conditions are like those in the manuscript.

Composition and structure – additional data

Table S1.
by ICP-MS of
some after
recalculated after

Material	Fe	C	O	N	Mg	Cl
A	25.8	70.7	3.2	0.3	0.0	0.0
B	33.1	49.4	15.7	0.9	0.9	0.0
C	2.9	87.9	8.3	0.3	0.6	0.0
D	45.2	44.0	7.8	3.0	0.0	0.0
E	74.7	25.1	0.2	0.0	0.0	0.0
A-wash	0.7	87.0	0.0	0.6	0.0	0.4
B-wash	6.2	86.5	0.0	0.7	0.1	2.0
C-wash	0.1	61.4	34.1	0.5	0.1	1.8
D-wash	2.2	95.7	0.0	1.5	0.0	0.6
E-wash	0.1	95.2	3.4	0.3	0.0	0.1

Elemental analysis
carbides **A–E** and
washing (in at%),
removing H₂O.

Table S2. Electrochemical surface areas.

Material	ECSA (m ² g ⁻¹)	ECSA increase factor, after wash
A	0.013	4698
A-wash	61.08	
B	0.24	141
B-wash	33.81	
C	5.31	1.2
C-wash	6.14	
D	0.68	19
D-wash	12.92	
E	0.3	11
E-wash	3.2	
GC	0.28	-

Table S3. Calculated binding energies for oxygen- and nitrogen-based intermediates (those presented in Figure 4 and others).

Adsorbed species	Adsorption energy on Pt(111) surface (eV)	Adsorption energy on Fe ₃ C surface (eV)
O ₂ (gas)	4.9	4.9
OOH	4.2	-2.89
O	1.6	-3.18
OH	0.85	-3.1
H ₂ O	0	0
N ₂ H ₄ (gas)	0.26	0.26
N ₂ H ₄	0.46	-1.15
N ₂ H ₃	0.945	-0.655
N ₂ H ₂	0.53	-1.22
N ₂ H	1.145	-2.11
N ₂	-0.3	-1.34
NH ₂	1.64	-2.04
N	0.50	-1.16
N ₂ (gas)	0	0

Material	N pyridinic (398.5-398.8 eV)	Fe-N _x (399.5-399.8 eV)	N pyrrolic (400.6-400.9 eV)	N quaternary (401.5-402.0 eV)	N graphitic (402.5-403.0 eV)
B-wash	17.57	39.55	18.84	18.84	5.21
D-wash	26.41	46.39	12.01	12.01	3.18

Table S4. Fractions of nitrogen types in B-wash and D-wash, from deconvoluted XPS in the N 1s region.

References

- 1 J. Park, K. An, Y. Hwang, J.-G. Park, H.-J. Noh, J.-Y. Kim, J.-H. Park, N.-M. Hwang and T. Hyeon, *Nat. Mater.*, 2004, **3**, 891–895.
- 2 D. C. Fletcher, R. Hunter, W. Xia, G. J. Smales, B. R. Pauw, E. Blackburn, A. Kulak, H. Xin and Z. Schnepf, *J. Mater. Chem. A*, 2019, **7**, 19506–19512.
- 3 O. Malina, P. Jakubec, J. Kašík, J. Tuček and R. Zbořil, *Nanoscale*, 2017, **9**, 10440–10446.
- 4 T. Danno, D. Nakatsuka, Y. Kusano, H. Asaoka, M. Nakanishi, T. Fujii, Y. Ikeda and J. Takada, *Cryst. Growth Des.*, 2013, **13**, 770–774.
- 5 C. Giordano, A. Kraupner, S. C. Wimbush and M. Antonietti, *Small*, 2010, **6**, 1859–1862.
- 6 C. Tang, W. Wang, A. Sun, C. Qi, D. Zhang, Z. Wu and D. Wang, *ACS Catal.*, 2015, **5**, 6956–6963.